Origin of molecular orbital splitting of C_{60} on Al(110)

2004 J. Phys.: Condens. Matter 16 L407

(http://iopscience.iop.org/0953-8984/16/36/L02)

INSTITUTE OF PHYSICS PUBLISHING JOURNAL OF PHYSICS: CONDENSED MATTER

J. Phys.: Condens. Matter **16** (2004) L407–L414 PII: S0953-8984(04)82148-9

LETTER TO THE EDITOR

Origin of molecular orbital splitting of C_{60} on Al(110)

J Schiessling[1,5], M Stener[2], T Balasubramanian[3], L Kjeldgaard[1,6], P Decleva[2], J Nordgren[1] and P A Brühwiler[1,4]

[1] Department of Physics, Uppsala University, Box 530, SE-751 21 Uppsala, Sweden
[2] Dipartimento di Scienze Chimiche, Universitá degli Studi di Trieste, Via L. Giorgieri 1, I-34127 Trieste, Italy
[3] Max-Lab, University of Lund, Box 118, SE-221 00 Lund, Sweden
[4] EMPA, Lerchenfeldstr. 5, CH-9014 St Gallen, Switzerland

E-mail: j.schiessling@phys.rug.nl and Paul.Bruehwiler@empa.ch

Received 15 June 2004
Published 27 August 2004
Online at stacks.iop.org/JPhysCM/16/L407
doi:10.1088/0953-8984/16/36/L02

Abstract

We have investigated the C_{60} monolayer on Al(110) with angle-dependent photoelectron spectroscopy. We find that orbital components have different angular distributions. Calculations of cross sections of the highest occupied molecular orbital components for free, oriented C_{60} are found to describe the experimental data quite well. The observed band splitting is attributed to intramolecular electronic correlations, due to the different coupling of the orbital components to the substrate conduction band.

(Some figures in this article are in colour only in the electronic version)

Molecule–surface interfaces constitute a key element in a vision of molecular electronics. An important goal in the application of molecules to electronics is the inclusion of relatively complex functionality within the molecule itself; this could be difficult to attain with an Å-scale molecule, but has been demonstrated for species similar in size to C_{60} [1, 2]. C_{60} has served as a prototype molecular device (component) [3–5] because of its symmetry, size, and ease of handling. For these device prototypes, the molecule–surface contact is a central issue [1, 2, 6, 7], and molecular correlation effects modified by the contact interactions are important [8]. A large database on the surface–fullerene interaction has been assembled in the literature [9], suggesting that this junction and its role in determining molecular functionality might be possible to control in the near future. The following substrate-dependent parameters of the fullerene–surface junction have emerged in previous work: the degree of charge transfer

[5] Present address: Materials Science Centre, University of Groningen, Nijenborgh 4, 9747 AG Groningen, The Netherlands.
[6] Present address: Max-Lab, University of Lund, Box 118, SE-221 00 Lund, Sweden.

(to the fullerene) [9–11], the importance of hybridization with the substrate [9, 12, 13], and the magnitude of charge–charge correlation effects [10, 14].

Hybridization and the concomitant energy level splitting [9, 12, 13, 15] is the aspect of the surface–fullerene interaction which could most strongly affect the use of such molecules in devices, since the level structure is often paramount to control. It has been claimed that the chemical rehybridization which is so well established for small molecular adsorbates [16] is also important for adsorbed C_{60} [17]. The large width of the molecule-derived levels has generally been attributed to substrate-induced hybridization effects [9, 12]. The fact that calculations in the local density approximation (LDA) produce single, rather than split, orbital manifolds for $C_{60}/Ag(001)$ can explain some of the broadening, but not the large splitting observed in the data [9]. At the same time, the similarity of the energy-dependent photoelectron cross sections of multi-and monolayer C_{60} films suggests that adsorption leaves the molecular levels largely unaffected [18]. The ability of simple calculations to reproduce x-ray photoelectron scattering data [19] implies only minor geometrical changes occur upon chemisorption. At the same time, isolated molecules of covalently bound [9, 20] C_{60}/Al are very mobile on the surface [21]. The roles of hybridization, vibrational coupling [22], and intramolecular correlation effects [10, 14] for such large molecules in contact with a surface are not yet generally understood.

We will use the angle dependence of the photoelectron spectrum (PES) of C_{60} to illuminate these issues for a system displaying some of the largest chemisorption-induced effects on the energy levels of the fullerene, $C_{60}/Al(110)$ [9]. The splitting of the highest occupied molecular orbital (HOMO) is confirmed to be due to the symmetry-breaking effect of the surface bond; the different components are assigned to orbitals which are degenerate for the free molecule via comparison of the angle dependence of their emission to calculations. The frontier orbital molecular wavefunctions can be classified into those with and without strong overlap with the substrate, suggesting that the difference in screening of an electron vacancy in these two cases explains the observed splitting. This is supported by comparison to other observables, including the magnitude of the electron–electron correlation energy for metal-supported C_{60} monolayers. This emphasizes the strong effect of single charges on such anchored molecules for the electronic structure.

The experiments were carried out at Beamline 33 at MAX-lab [23], which has an angle-resolved photoelectron spectrometer in a standard ultrahigh vacuum chamber, connected to a sample preparation chamber via a transfer system. The angular resolution was 2°, and the base pressure during measurements 6×10^{-11} mbar. The ordered monolayer was formed by subliming C_{60} onto the clean (110) surface while the substrate was held at 620 K. The experimental geometry and the low energy electron diffraction (LEED) pattern are shown in figure 1. Further experimental details on the sample preparation will be reported in detail elsewhere [24]. All data shown here were acquired at 32 eV photon energy with the polarization in the plane of incidence at an angle of 25° from normal. The Al(110) surface was oriented to place the [10] direction in this plane. The spectral intensity was normalized to the total photon flux during acquisition. The differential photoionization cross section has been calculated using an approach which combines density functional theory with a basis consisting of a large one-centre expansion (OCE) of products of radial B-spline functions and symmetry adapted spherical harmonics; see [25–27] for more details. In the present work we employ a conventional Kohn–Sham Hamiltonian [28], with the LB94 exchange–correlation potential [29]. The complete I_h point group symmetry has been employed in the calculations.

Valence data from $C_{60}/Al(110)$ are shown in figure 2(a); the binding energy scale is shown on the top axis, and the kinetic energy of the photoelectron on the bottom axis. The kinetic energy is determined by the energy difference between the calibrated photon energy and the work function of $C_{60}/Al(110)$ [30]. The data show a strong splitting of the highest occupied

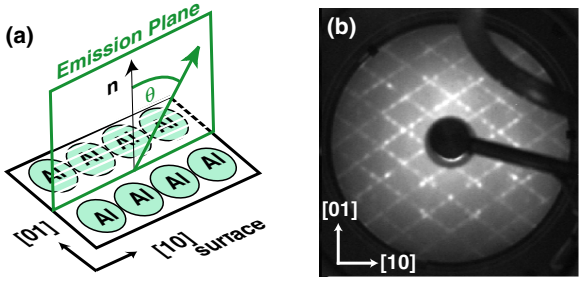

Figure 1. (a) Illustration of the experimental geometry. (b) Observed LEED pattern. The surface directions are indicated.

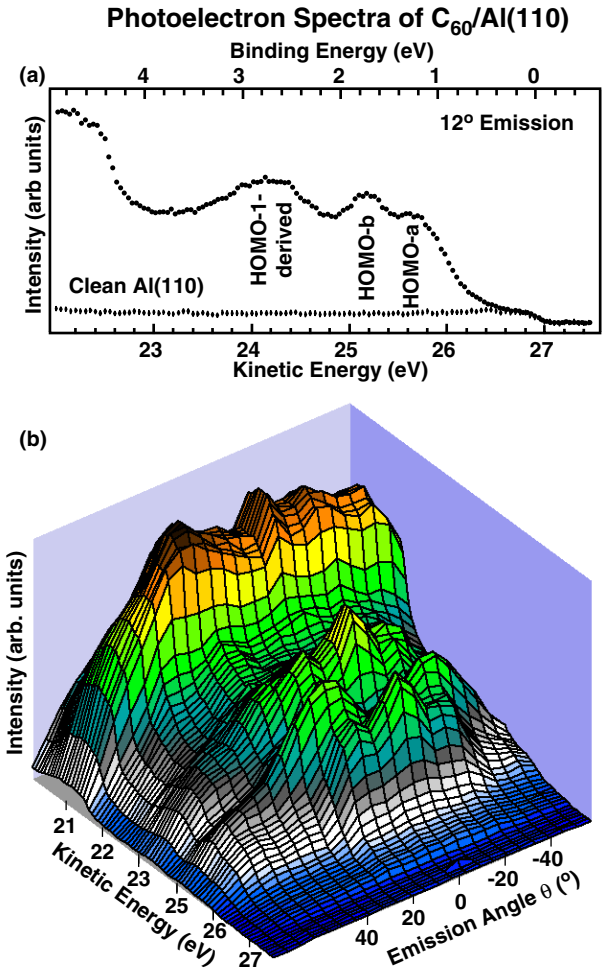

Figure 2. (a) A single spectrum and (b) an ensemble of angle-dependent valence PESs of C_{60}/Al(110). The spectra in (b) were taken at 6° intervals, indicated by the lines.

molecular orbital (HOMO) [9] into two components, 'a' and 'b'; note that the Al background is quite weak in comparison to the fullerene-derived features. A set of valence spectra for a

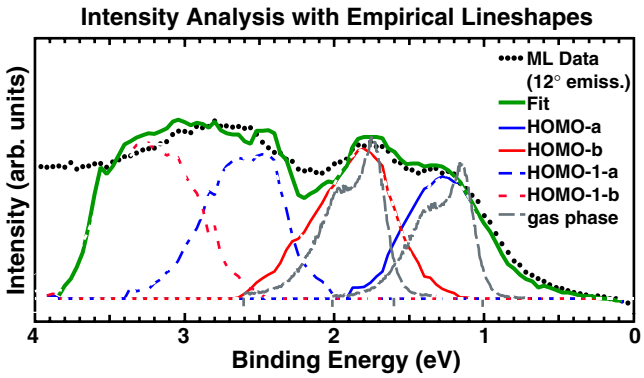

Figure 3. Illustration of the fitting procedure used to extract the angle dependence shown in figure 4 from the data in figure 2(b); the background due to the substrate has been subtracted. Grey dashed curves show the HOMO band of gas phase C_{60} [22] for comparison to the empirical component lineshapes.

range of polar emission angles is shown in figure 2(b), displaying a rich intensity variation throughout the selected energy range. We focus in what follows on the HOMO, which is derived from a single molecular orbital and shows the strongest angle dependence, allowing a detailed analysis.

To extract the form of each angle dependence, we first scaled and subtracted spectra at different angles from each other to determine empirical lineshapes for each component, as well as for the band below (HOMO-1). These are shown in figure 3; the quality of fit shown there was found for all angles, and further details are given elsewhere [24]. The results of fitting the empirical lineshapes to the HOMO-a and HOMO-b are shown at the bottom of figure 4. Consistent with figure 2(b), HOMO-a has an intensity maximum at normal emission and shoulders at about $\pm 20°$. HOMO-b is characterized by a local minimum at normal emission and structures at $\pm 25°$. We denote the peaks at $\pm 20°$ and $\pm 25°$ as 'wing structures'.

The molecular appearance of the variations suggests, as with the energy dependence [18], that a calculation for an isolated, oriented molecule could explain the data. The orientation for C_{60} on the similarly structured surfaces Cu(110) [19, 31] and Pd(110) [32] was experimentally determined to be characterized by five to six bonds in contact with the surface, aligned perpendicularly to the rows of substrate atoms.

To test this, we compare the experimental angle dependences to calculations for each of a set of allowed molecular orientations in figure 4. We make the ansatz that a twofold axis of symmetry of the molecule will be aligned to one of the substrate twofold axes. For cases in which the molecule has no mirror plane perpendicular to the emission plane, the two equivalent orientations are included in the calculation (see figure 5(a)). Emission in a mirror plane as nominally required by the experimental geometry employed here eliminates contributions from several of the five HOMO components [33] due to symmetry considerations; hence only the symmetry-allowed contributions are displayed. The calculated distributions are corrected for electron refraction, increasing spot size collected by the analyser at higher emission angles, and attenuation due to inelastic scattering [34]. They have then been broadened with an 8° wide Gaussian to simulate the width of the experimentally determined structures, and compressed in the angular dimension by a factor of 1.4, which was found [24] to bring the solid C_{60} data [34] into agreement with calculations.

Almost all orientations can be eliminated after a cursory comparison of the predicted angular distributions to experiment. Cases (a), (b), (f), (g), (h), (i) and (j) all predict overly

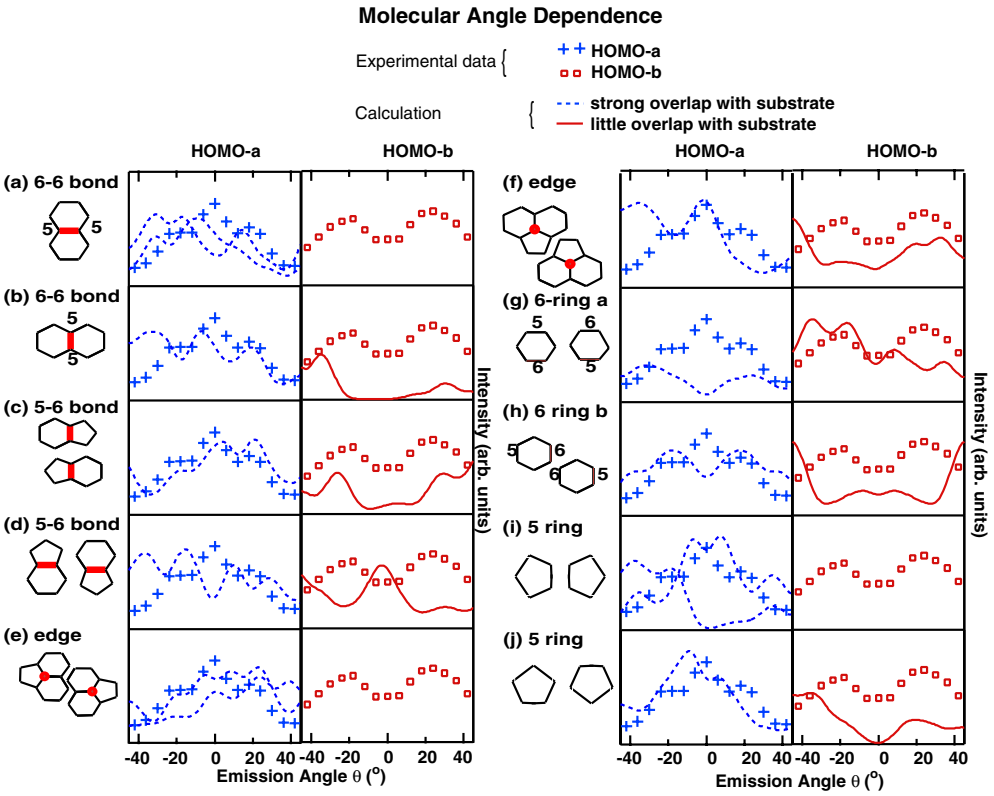

Figure 4. Left columns: schematics of the molecular orientation, taking the surface [10] direction to be horizontal. The bond or atom closest to the Al surface is drawn as a thick line or circle, respectively. Right columns: corresponding calculated photoelectron angular distributions for emission in the experimental emission plane, compared to the experimental curves. See the text for discussion.

high intensity at greater emission angles. For geometry (d) the component distribution with significant intensity at normal emission has only weak wing structures, and at very high emission angles, in contrast to HOMO-a. Case (e) shows rather uniform distributions, unlike the experiment. The remaining possibility (c) has only one component with significant intensity at normal emission, and both components show wing structures; this and the relative placement of those structures (HOMO-b further apart than HOMO-a) is in quite good agreement with experiment. Thus, calculations based on isolated molecules identify orientations with five to six bonds in contact with the surface and aligned to the [01] direction as the only reasonable case of those considered. This is in excellent agreement with the experimentally determined orientations for C_{60} on Cu(110) [19, 31] and Pd(110) [32]. Indeed, in all studies so far, the surface symmetry plays the deciding role for the molecular orientation [24]. This supports the use of a free molecular calculation, and strongly suggests that the molecular orbitals are only weakly mixed with substrate states upon chemisorption on Al(110).

The fact that two components are observed here and for angle-integrated data taken with a less restrictive surface-emission orientation [9] suggests that the observed splitting is not merely a consequence of emission symmetry, which could be expected to divide the fivefold degenerate HOMO into at least three separate components in the ground state, or broaden it

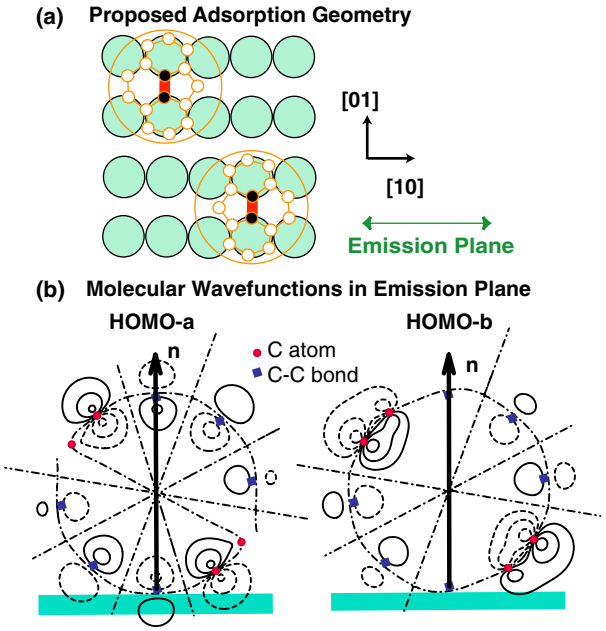

Figure 5. (a) Molecular orientation(s) of C_{60}/Al(110) consistent with the comparison shown in figure 4, and with expectations from structure studies (see text). Only the carbon atoms closest to the surface are shown explicitly. The C–C bond closest to the substrate is indicated as a solid line. The adsorption site depicted is arbitrary. (b) Contour plot of the wavefunctions of the components corresponding to figure 4(c). Portions with positive (negative) phase are shown as solid (dashed) lines, and the nodal lines as dash–dotted lines. Circles show C atom positions, while the squares indicate the intersection between the emission plane and C–C bonds. The substrate and the surface normal are also indicated. The emission plane is a nodal plane for three out of the five HOMO-derived components in this geometry.

into a continuum according to theory [12]. The overlap of the different HOMO components with the substrate, illustrated schematically in figure 5(b), offers a simple explanation for the existence of exactly two components. There we see that the HOMO-a and HOMO-b have relatively strong and quite small overlap with the substrate, respectively. This difference in overlap characterizes the other three components of the HOMO as well, and motivates the energy-splitting in terms of a final state effect.

To estimate the splitting, we note that the photohole created on the molecule in the measurement will be fully localized there for components like HOMO-b, but will be delocalized into the substrate to some extent for components like HOMO-a. In the extreme case, this would leave the molecule with local charges of +1 and 0, respectively, and the difference in energy cost, i.e., the splitting sought here, would be the self-energy of a single charge on an adsorbed fullerene, which explains its absence in ground state calculations [12]. This should be about half the charge–charge correlation energy U, which has been found to be 0.6 eV for C_{60}/Ag(111) [14], i.e., a maximum splitting of about 0.3 eV for adsorption on a metal, which is quite close to the value found here. For semiconductor substrates this splitting would be expected to increase somewhat due to the reduced image screening, as observed [13, 15]. Thus the splitting can to a good approximation be explained in terms of the difference in hole correlation energy between orbitals with and without significant substrate overlap.

From the previous study of C_{60}/Al [9], we identify the HOMO-a component as that displaying significant substrate overlap, based on the fact that the HOMO-b is virtually

unchanged as the substrate is varied, whereas the HOMO-a showed signs of varying extent of substrate hybridization. This observation motivates the coloring of the curves in figure 4: angular distributions from components with relatively large substrate overlap are given in blue, those with virtually no substrate overlap in red. With this additional criterion, we obtain further confirmation of our previous analysis; e.g., cases (a) and (e) are eliminated due to the lack of a red component, and case (d) because the red component has a central maximum. Case (c) is once again shown to satisfy the available constraints.

All the new observations in the present work are attributable to the retention of significant molecular character by the electronic states of the fullerene upon adsorption. The strong similarity between the HOMO-a and HOMO-b lineshapes shown in figure 3 and that of gas phase C_{60} indicates that vibrational coupling, which is suggested to be significant in solid C_{60} [10, 22, 35], could play an important role in the level widths. The close similarity of the weakly coupled component HOMO-b with the gas phase data, and the extra broadening of the HOMO-a relative to those data, are consistent with the stronger substrate interaction of the HOMO-a component, and with the strong molecular character deduced from the angle dependence.

This would also help to explain the overlap of the HOMO-a and HOMO-b components without the need to invoke a strong substrate interaction for both components. The hybridization effects elucidated in [12] are important for the orbitals which are involved, but cannot explain the splitting observed. Hence we speculate that vibrational coupling is an important contributing factor in explaining why level splitting of the type described here and elsewhere [8] is not evident in C_{60}-based prototypical devices studied to-date [3, 4].

To summarize, we have used the angular distribution of the adsorption-split components of the highest occupied molecular orbital of C_{60}, combined with calculations for the free molecule, to identify the sub-orbitals involved. This has led to a molecular picture of the major aspects of the adsorbate electronic structure, with only minor modifications due to the covalent bond to the surface. The splitting of the HOMO, which is obvious for several other substrates as well, is explained in terms of differences in correlation energy of the final state as a function of differing covalent interactions of the sub-orbitals involved. The present results have general implications for molecular devices in which a covalent bond between molecule and substrate is important for electronic applications.

We gratefully acknowledge experimental assistance from K Hansen, as well as funding from Vetenskapsrådet and the CARAMEL Consortium, which receives funding from Stiftelsen för Strategisk Forskning. LK acknowledges support from Statens Naturvidenskabelige Forskningsråd, Denmark.

References

[1] O'Regan B and Grätzel M 1991 *Nature* **353** 737
[2] Derycke V, Martel R, Appenzeller J and Avouris P 2001 *Nano Lett.* **1** 454
[3] Joachim C, Gimzewski J K and Aviram A 2000 *Nature* **408** 541
[4] Park H *et al* 2000 *Nature* **407** 57
[5] Theobald J A *et al* 2003 *Nature* **424** 1029
[6] Schnadt J *et al* 2002 *Nature* **418** 620
[7] Javey A *et al* 2003 *Nature* **424** 654
[8] Kubatkin S *et al* 2003 *Nature* **425** 698
[9] Maxwell A J *et al* 1998 *Phys. Rev.* B **57** 7312
[10] Rudolf P, Golden M S and Brühwiler P A 1999 *J. Electron. Spectrosc. Relat. Phenom.* **100** 409
[11] Cepek C *et al* 2001 *Phys. Rev. Lett.* **86** 3100
[12] Lu X *et al* 2003 *Phys. Rev. Lett.* **90** 096802

[13] Bertoni G, Cepek C and Sancrotti M 2003 *Appl. Surf. Sci.* **212** 52
[14] Hesper R, Tjeng L H and Sawatzky G A 1997 *Europhys. Lett.* **40** 177
[15] Sakamoto K *et al* 1998 *Phys. Rev.* B **58** 13951
[16] Hoffmann R 1988 *Rev. Mod. Phys.* **60** 601
[17] Veenstra S C *et al* 2002 *Appl. Phys.* A **75** 661
[18] Ton-That C *et al* 2003 *Phys. Rev.* B **67** 155415
[19] Fasel R *et al* 1996 *Phys. Rev. Lett.* **76** 4733
[20] Stengel M, Vita A D and Baldereschi A 2003 *Phys. Rev. Lett.* **91** 66101
[21] Johansson M K *et al* 1998 *Surf. Sci.* **397** 314
[22] Brühwiler P A *et al* 1997 *Chem. Phys. Lett.* **279** 85
[23] Jensen B N *et al* 1997 *Nucl. Instrum. Methods Phys. Res.* A **394** 243
[24] Schiessling J *et al*, unpublished
[25] Venuti M, Stener M and Decleva P 1998 *Chem. Phys.* **95** 234
[26] Venuti M, Stener M, Alti G D and Decleva P 1999 *J. Chem. Phys.* **111** 4589
[27] Colavita P *et al* 2002 *Phys. Chem. Chem. Phys.* **3** 4481
[28] Parr R G and Yang W 1989 *Density Functional Theory of Atoms and Molecules* (New York: Oxford University Press)
[29] van Leeuwen R and Baerends E J 1991 *Phys. Rev.* A **49** 2421
[30] Maxwell A J *et al* 1996 *Chem. Phys. Lett.* **260** 71
[31] Fasel R, Agostino R G, Aebi P and Schlapbach L 1999 *Phys. Rev.* B **60** 4517
[32] Weckesser J *et al* 2001 *J. Chem. Phys.* **115** 9001
[33] Wästberg B and Rosén A 1991 *Phys. Scr.* **44** 276
[34] Schiessling J *et al* 2003 *Phys. Rev.* B **68** 205405
[35] Shirley E L, Benedict L X and Louie S G 1996 *Phys. Rev.* B **54** 10970